

Effects of index mismatch induced spherical aberration on two-photon imaging in skin and tissue-like constructs

(Invited Paper)

Chih-kuan Tung^a, Tsung-Kai Chiu^a, Wen Lo^a, Po-Hsiang Wang^{a&},
Sun-Jan Lin^b, Shiou-Hwa Jee^{b,c}, Chen Yuan Dong^{a*}

^aDept. of Physics, National Taiwan University, Taipei 106, Taiwan, Republic of China

^bDept. of Dermatology, National Taiwan University Hospital, Taipei 106, Taiwan,
Republic of China

^cDept. of Dermatology, National Taiwan University College of Medicine, Taipei 106, Taiwan,
Republic of China

Abstract

Index mismatch induced spherical aberration is studied by comparing imaging ability of different immersion objectives in both uniformly fluorescent solutions and fluorescently labeled skin samples using scanning two-photon fluorescence microscopy. We investigated the performances of the objectives (air, water, glycerin, and oil immersion) by measuring the fluorescence profiles at different depths. In homogeneous fluorescent samples, we found that immersion medium with compatible refractive index as the samples yields better results, and small differences in refractive indices did not cause noticeable effects. Similar results were found in skin samples. Except for the air objective, we found that the choice of immersion medium did not have significant effects for in-depth imaging in the fluorescent solutions or skin samples.

Keywords: two-photon, fluorescence, microscopy, skin, imaging, spherical aberration

1. Introduction

Two-photon fluorescence microscopy (TPFM) is a powerful, three-dimensional imaging technique. Since the near-infrared photons used for sample excitation are absorbed and scattered less than the UV or visible photons used in confocal microscopy, TPFM allows the imaging of biological specimens to greater depths than single-photon confocal microscopy¹⁻³. With its quadratic dependence of the fluorescence excitation efficiency, the excitation volume of TPFM is confined to near the focal spot¹. As a result, axial depth discrimination becomes greatly enhanced and sample photodamage greatly reduced¹. In addition, the nature of the two-photon excitation keeps the emission wavelength far from the excitation wavelength, thus allowing superior imaging sensitivity³. TPM can also be used to initiate photochemical reaction within a sub-femtoliter volume^{1,3}.

The in-depth imaging capability of TPFM implies that serious spherical aberration may occur when we use TPFM to image deep within tissues. The refractive index differences in different parts of the same tissue specimen can result in spherical aberration leading to image degradation⁴.

*Address correspondence to: E-mail: cydong@phys.ntu.edu.tw; Telephone: +886(2)3366-5155; Fax: +886(2)3366-5196

&Current address: Institute of Applied Science & Engineering Research, Academia Sinica, Taipei 115, Taiwan, Republic of China

Index-mismatch induced spherical aberration occurs naturally when imaging deep in skin samples. The surface of the skin is more oil-like with a refractive index of 1.47. This value decreases in the upper epidermal layer to 1.43 (granular layer) and eventually becomes close to that of water (1.34) in the basal layer. In the upper dermis, the refractive index again increases to around 1.41^{5,6}. This type of refractive indices mismatch can enlarge the focal volume, and induces an axial focal shift^{4,7}.

In examining physiological specimens, two-photon microscopy has been widely applied to skin imaging^{8,9,10}. In addition to morphological and spectroscopic imaging^{8,9}, TPFM has also been used in transdermal drug delivery studies to visualize the transport of fluorescent molecules¹⁰. In these studies, it is often needed to quantitatively determine the axial concentrations profiles of fluorescent molecules. However, refractive index mismatch induced spherical aberration can lead to inaccuracy in the determination of fluorophore concentration in depth. In particular, the quadratic dependence of two-photon excitation efficiency means that the fluorescence generated at the TPFM focal spot is sensitive to any degradation in the point-spread-function. Factors such as specimen turbidity and spherical aberration can both lead to a decrease in measured fluorescence intensity. In this work, we focus on investigating the effects of spherical aberration induced effects by comparing the performance of objectives under different immersion fluids in two-photon imaging of excised skin.

2. Experimental methods

2.1 Two-photon microscopic instrumentation

The experimental setup is based on a Nikon E800 upright microscope, similar in arrangement to a system described previously³. Excitation light source used in the experiments is a pulsed, femtosecond titanium-sapphire laser (Tsunami, Spectra-Physics, Mountain View, CA) pumped by a 10W, 532 nm diode laser system (Millennia, Spectra Physics). After attenuation by a pair of half wave plate and polarizer, the beam is scanned by galvanometer-drives x-y mirrors (Model 6220, Cambridge Technology, Cambridge, MA). The beam is then expanded by a pair of lenses to ensure over-filling of the objectives' back aperture. The objectives we used include an air objective (20x S Fluor, NA 0.75, Nikon, Japan), a multi-immersion (water, glycerol, and oil) objective (20x Plan Fluor, NA 0.75, Nikon), a high NA water-immersion lens (60x Plan Apo, NA 1.2, Nikon), and a high NA oil-immersion objective (60x Plan Apo, NA 1.4, Nikon). These objectives enable us to compare the effects of numerical aperture and immersion medium in two-photon imaging applications. Axial scanning is achieved using a motorized focus control (ProScan, Prior Scientific, UK). The emission fluorescence is collected by the same objective, split from the excitation light by a dichroic mirror and a short pass filter, before being detected by a single-photon counting, photomultiplier tube (R7400P, Hamamatsu, Japan). By counting photon signals from PMT, we can obtain the two-photon fluorescence intensity at each point in the sample. The galvanometric mirrors, focus, and PMT signal processing are controlled by a PC program.

2.2 Samples preparation and imaging

The fluorescent probe, sulforhodamine B (SRB, R-634, Molecular Probes, Eugene, OR) was used in both water, glycerine and skin samples. The SRB water and glycerine solutions were prepared at concentrations of 0.5mg SRB per ml. The solution is placed into a well-microslide and sealed with a cleaned No. 1.5 coverglass. The skin from the chest area acquired 3-4 hrs after surgical operation, was stored at buffer solution at -20 °C and utilized within 2 weeks. The fluorescent solution for skin sample consisting of ethanol (100%, Sigma, St. Louis, MO) and PBS (0.01M phosphate buffer, 0.0027 M KCl and 0.137 NaCl, pH=7.4; Sigma), at a 1:1 ratio and 5% oleic acid (O-1008, Sigma), by volume, was prepared at concentration of 0.5mg SRB per ml. Skin samples were dipped in fluorescent solution for 48hrs, rinsed with PBS and blotted with a Kimwipe to eliminate excess fluorescent probes present on the surface of the skin. The skin was sealed in a well-microslide with a No. 1.5 coverglass. A twisted Kimwipe tissue soaked in PBS was placed under the skin to prevent the sample from drying out and to support the skin against the coverglass.

Each sample was observed by all four objectives. Since spherical aberration is induced by refractive indices mismatch, immersion media with different refractive indices will help us to understand the effect of spherical aberration. Refractive indices of the immersion media at 656.3 nm are, 1.3312 of water, 1.4672 of glycerine, 1.5127 of oil¹¹. Compared with the value of 1.5143 for glass¹¹, surface between immersion medium and coverglass, and between coverglass and sample will both induce spherical aberration. Since 20x S Fluor and 60x Plan Apo oil objectives are designed for #1.5 coverglass (thickness 0.17 mm), the effects of coverglass in the above cases are minimal. In 20x Plan

Fluor and 60x Plan Apo water cases, the correction collar on the objectives can be adjusted to correct for variations in coverglass thickness.

In comparing the performance of different objectives in skin imaging, we need to image the same region of the skin specimen. This was achieved by turning up the laser intensity and marking a region of the skin using the bubbles created from photodamage.

3. Results

3.1 Intensity profile in homogeneous samples

Since spherical aberration can degrade both the radial and axial point-spread-function (PSF), the measured fluorescence can decrease as a function of depth. To investigate this effect, we measured the axial intensity profiles in a homogeneous fluorophore sample. By imaging fluorophores dissolved in solvents with different refractive indices, we can investigate the effect of PSF degradation. The first experiment we performed was to compare the axial intensity profiles of the SRB dissolved in water sample obtained using the 20x air, water, glycerin, and oil immersion objectives and the results are shown in Fig. 1.

In the case of the water sample, we found that the air objective produced the most pronounced effects of index mismatch induced spherical aberration. For example, at 100 microns depth from the surface, the intensity dropped 62% for the air objective, and 36%, 28%, 26% for the glycerine, oil, water objectives, respectively.

Similar observation was observed when we perform the same experiments on a glycerine sample. In Fig. 2, one finds that the air immersion objective still showed the largest extent of spherical aberration, and the axial intensity profiles obtained using other objectives differ little from each other. Compared to the surface intensity, the measured fluorescence intensity dropped by 70%, 20%, 20%, and 13% when air, glycerine, oil, water objectives are respectively used. The above results indicate that at the imaging depth of 100 microns, the use of an air immersion objective can result in more than twice the intensity reduction.

We also repeated the SRB solutions experiments with the 60x water and oil immersion objectives and the results are shown in Fig. 3. As Fig. 3 shows, for the SRB water sample, the axial fluorescence intensity profile obtained using a water-immersion objective suffered the least amount of fluorescence intensity decay. Comparing the intensity at a depth of 70 microns, the measured fluorescence decayed by: 25% for the water–water (immersion – sample) case, 22% for the oil – glycerine case, 48% for the water – glycerine case, and 56% for the oil – water case. In these cases, the water – water and oil – glycerine interfaces suffer the least amount of spherical aberration. Compared with 20x cases, the differences in using the 60x water and oil lenses are not as large as differences between a 20x air immersion and other 20x objectives using different immersion fluids. In addition, in most cases, the intensity reduction in a glycerin sample is less than that in a water sample. It is possible that the glycerin samples suffer less spherical aberration from coverglass to sample interface than for the water specimens. Furthermore, our results indicate that the spherical aberration was not fully corrected in our experiments. It is possible that the coverglass correction collar needs additional fine adjustments. This may be the explanation why the measured fluorescence profile in the oil–glycerine case showed slightly lesser effects due to spherical aberration than in the water – water case.

In a previous work, it has been calculated that lower numerical aperture objective suffers less spherical aberration⁷. This observation is consistent with our experimental results. Fig. 4 shows that regardless of the type of immersion objective and the sample solvent used, the axial intensity profile obtained using a lower NA objective showed less intensity reduction as imaging depths are increased. At a depth of 70 microns, the oil immersion objective and glycerin sample (oil – glycerin), intensity decreases 14% for the 20x objective, and 32% for the 60x lens. In the oil – water case, intensity reduction is 20% for the 20x objective and 56% for 60x lens. For the water – glycerin experiment, 7% reduction for the 20x lens and 48% for 60x objectives were observed. Finally, the water – water situation yielded 19% reduction for the 20x lens and 25% decrease for the 60x objective.

With above results, we can conclude that immersion medium with similar refractive index as the sample can minimize the effect from spherical aberration, and that the data acquired with the air objective (maximum difference in refractive indices with the samples) showed the greatest effects due to spherical aberration. Furthermore, at the same imaging depth, a lower NA objective demonstrated a less degree of spherical aberration compared to an objective with higher NA.

3.2 Immersion comparison in two-photon skin imaging

Unlike the case of a sample with uniform refractive index, the choice of immersion objective for two-photon skin imaging is less obvious. As a stratified medium, a description of spherical aberration in skin is more complicated than in two-medium interface⁴. The refractive indices of the skin vary from the surface stratum corneum, into the deeper epidermal layers, and again changes in the upper dermis^{5,6}. To investigate spherical aberration in the skin, we decided to measure and compare the intensity profiles of SRB treated skin using the same sets of 20x and 60x objectives used for obtaining the axial intensity profiles in SRB/water and SRB/glycerin samples. The SRB treated skin specimens are of particular interests since SRB has been used as a model system in transdermal drug delivery studies¹⁰. Since the skin is a heterogeneous sample, the fluorescent probes will most likely not be uniformly distributed in the skin. Nonetheless, we can still compare the intensity decay using different objectives provided that the same area of the skin is imaged.

Images of the skins under 20x objectives are shown in Fig. 5 a)-d), and the corresponding depth profiles are shown in the upper part of Fig. 6. A set of representative images in the upper epidermis (Fig. 5) is shown for comparison. To evaluate the relative effects of spherical aberration under different immersion objectives, one needs to compare the axial intensity profiles. From Fig. 6, one can see that at the same imaging depth, the air objective measured less fluorescence than the other immersion objectives. Among the water, glycerin, and oil immersion objectives, the axial intensity profiles are comparable. Compared with the surface intensity maximum, at a depth of 15 microns, an air immersion objective provides a 93% intensity reduction, and that value for different immersion fluids are glycerin: 78%, oil: 78%, water: 80%.

Similar experiments were performed on the 60x objectives, and the images are shown in Fig. 5 e), f). The corresponding fluorescence depth profiles are shown in Fig. 6. As in the case for the multi-immersion 20x objective, oil and water immersion lenses yielded comparable depth profiles, indicative of the fact that both immersion objectives perform comparably in two-photon skin imaging. At an imaging depth of 15 microns, the water lens yields 93% intensity reduction than the maximum value and oil yields a 90% reduction.

4 Conclusions

In this work, we compared the performances of objectives with different NA under different immersion conditions (air, water, glycerin, and oil) in the imaging of uniform SRB/water, SRB/glycerin, and SRB treated skin specimens. In all cases, the air objective showed the largest amount of spherical aberration, and the other type of immersion conditions (water, glycerin, oil) yielded comparable axial intensity fluorescence profiles. Furthermore, lower numerical aperture objectives showed a lesser degree of spherical aberration. Since our results are based on the measured depth intensity profiles, we feel that a more complete study would involve measuring the PSF in the specimens used in this work.

Acknowledgement

We like to thank Prof. Peter T. C. So's group (Department of Mechanical Engineering, MIT) for helping us in setting up the two-photon microscope system. This work is supported by NSC 90-2112-M-002-054 and NSC 91-2112-M-002-202 (provided by National Science Council, Taiwan, R.O.C.).

References

1. W. Denk, J. H. Strickler, and W. W. Webb, "Two-photon laser scanning fluorescence microscopy," *Science*, **248**, pp. 73-76, 1990.
2. V. E. Centonze and J. G. White, "Multiphoton excitation provides optical sections from deeper with scattering specimens than confocal imaging," *Biophys J.* **75**, pp. 2015-2024, 1998.
3. P. T. C. So, C. Y. Dong, CY, B. R. Masters, and K. M. Berland, "Two-photon excitation fluorescence microscopy," in *Annual Review of Biomedical Engineering*, volume 2, pp. 399-429. Annual Reviews, Palo Alto, 2000.

4. P. Török and P. Varga, "Electromagnetic defraction of light focused through a stratified medium," *Appl. Opt.* **36**, pp. 2305-2312, 1997.
5. G. J. Tearney, M. E. Brezinski, J. F. Southern, B. E. Bouma, M. R. Hee, and J. G. Fujimoto, "Determination of the refractive index of highly scattering human tissue by optical coherence tomography," *Opt. Lett.* **20**, pp. 2258-2260, 1995.
6. A. Knüttel and M. Boehlau-Godau, "Spatially confined and temporally resolved refractive index and scattering evaluation in human skin performed with optical coherence tomography," *J. Biomedical Optics.* **5**, pp. 83-92, 2000.
7. P. Török, P. Varga, and G. R. Booker, "Electromagnetic diffraction of light focused through a planar interface between materials of mismatched refractive indices: structure of the electromagnetic field. I," *J. Opt. Soc. Am. A* **12**, pp. 2136-2144, 1995.
8. B. R. Masters, P. T. C. So, and E. Gratton, "Multiphoton excitation fluorescence microscopy and spectroscopy of in vivo human skin," *Biophys. J.* **72**, pp. 2405-2412, 1997.
9. P. T. C. So, H. Kim, and I. E. Kochevar, "Two-photon deep tissue ex vivo imaging of mouse dermal and subcutaneous structures," *Opt. Exp.* **3**, pp. 339-350, 1998.
10. B. Yu, C. Y. Dong, P. T. C. So, D. Blankchtein, and R. Langer, "In vitro visualization and quantification of oleic acid induced changes in transdermal transport using two-photon fluorescence microscopy," *Journal of Investigative Dermatology*, **117**, pp. 16-25, 2001.
11. M. Pluta, *Advanced Light Microscopy* vol. 1, pp. 57, Elsevier, New York, 1988.

20x, water sample, immersion comparison

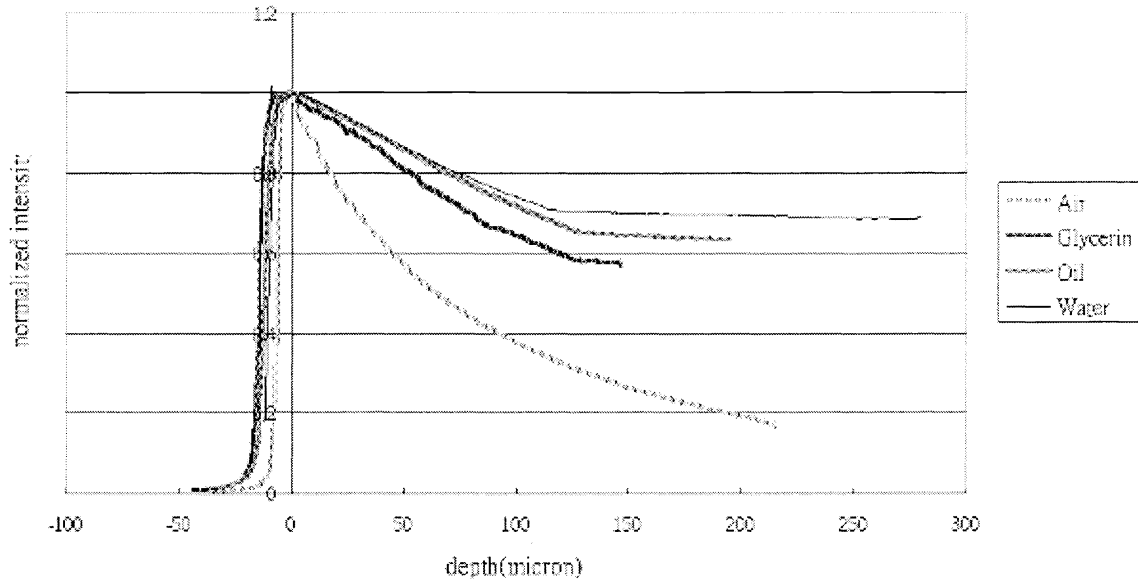


FIG. 1 Intensity profiles of water samples by 20x objectives.

20x, glycerine sample, immersion comparison

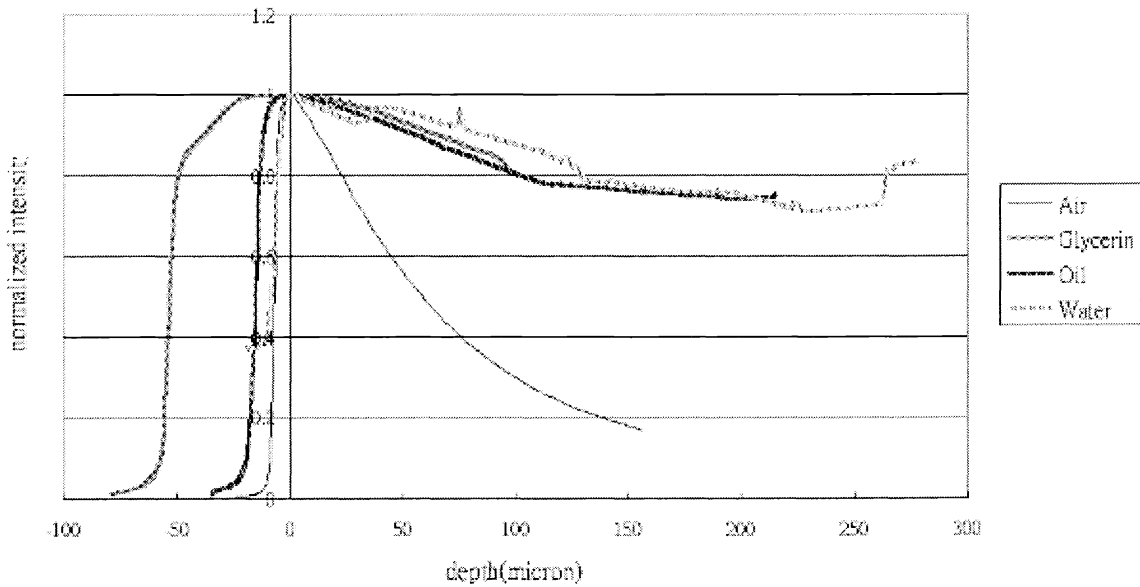


FIG. 2 Intensity profiles of glycerine samples by 20x objectives.

60x immersion comparison

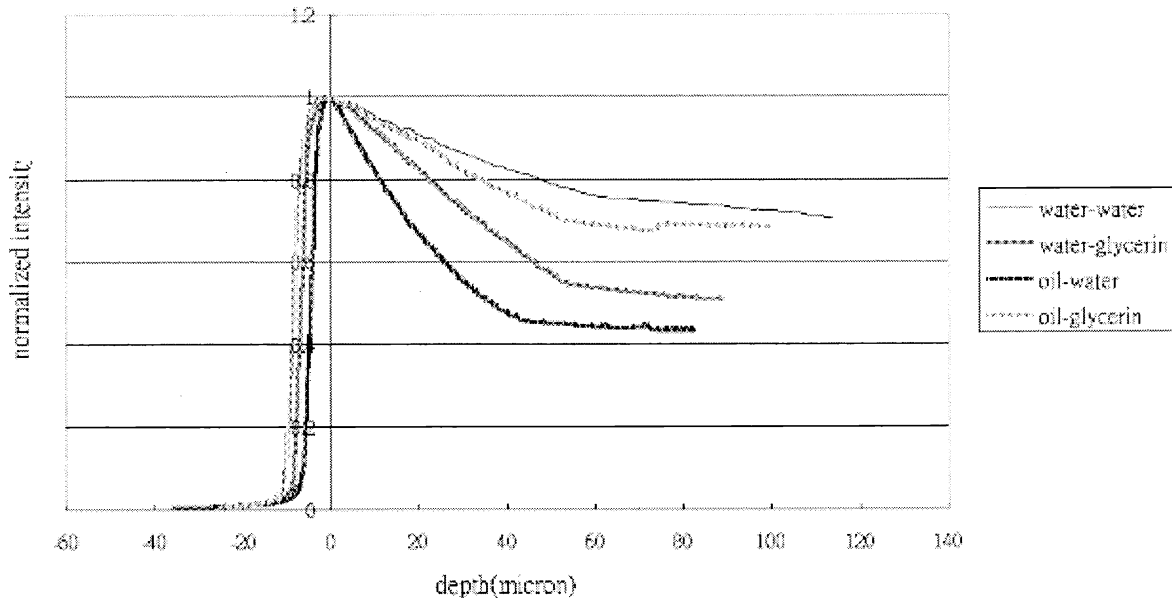
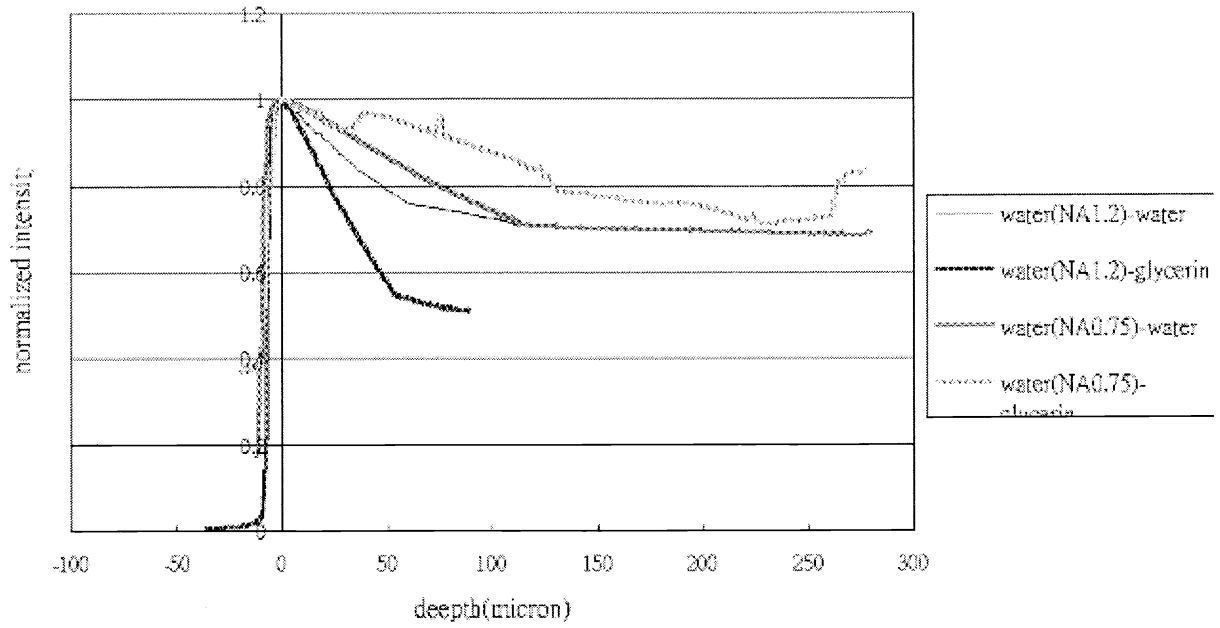


FIG. 3 Intensity profiles of 60x objectives. Line style explanation: immersion medium – sample medium.

Water immersion NA comparison



Oil immersion NA comparison

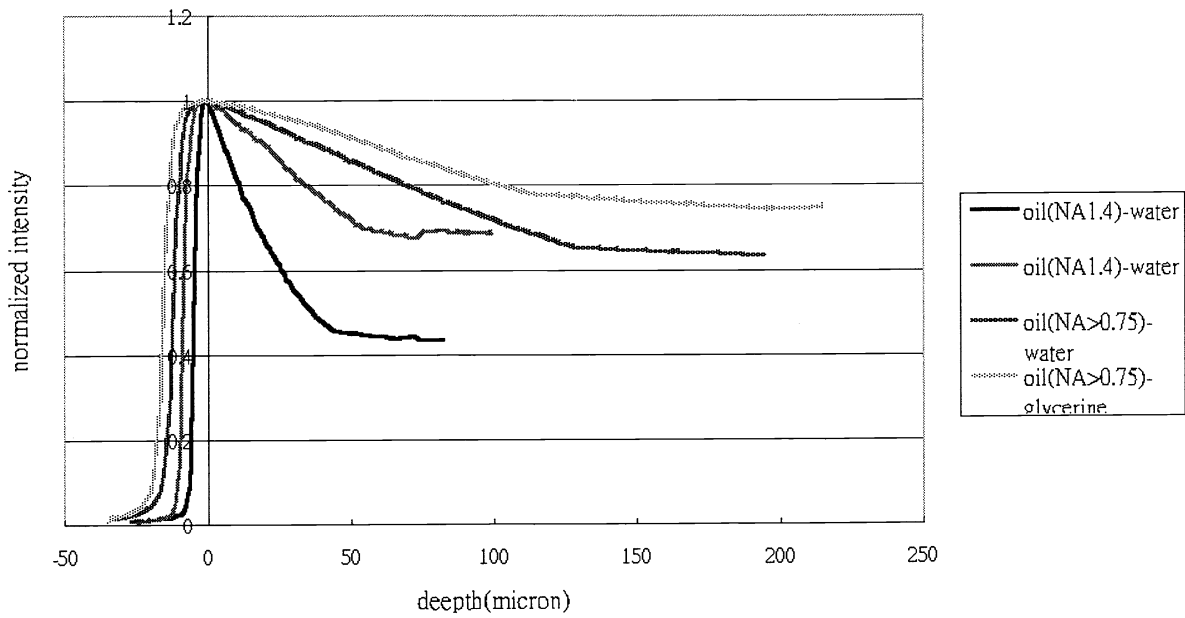


FIG. 4 Numerical comparison of water and oil immersion objectives.

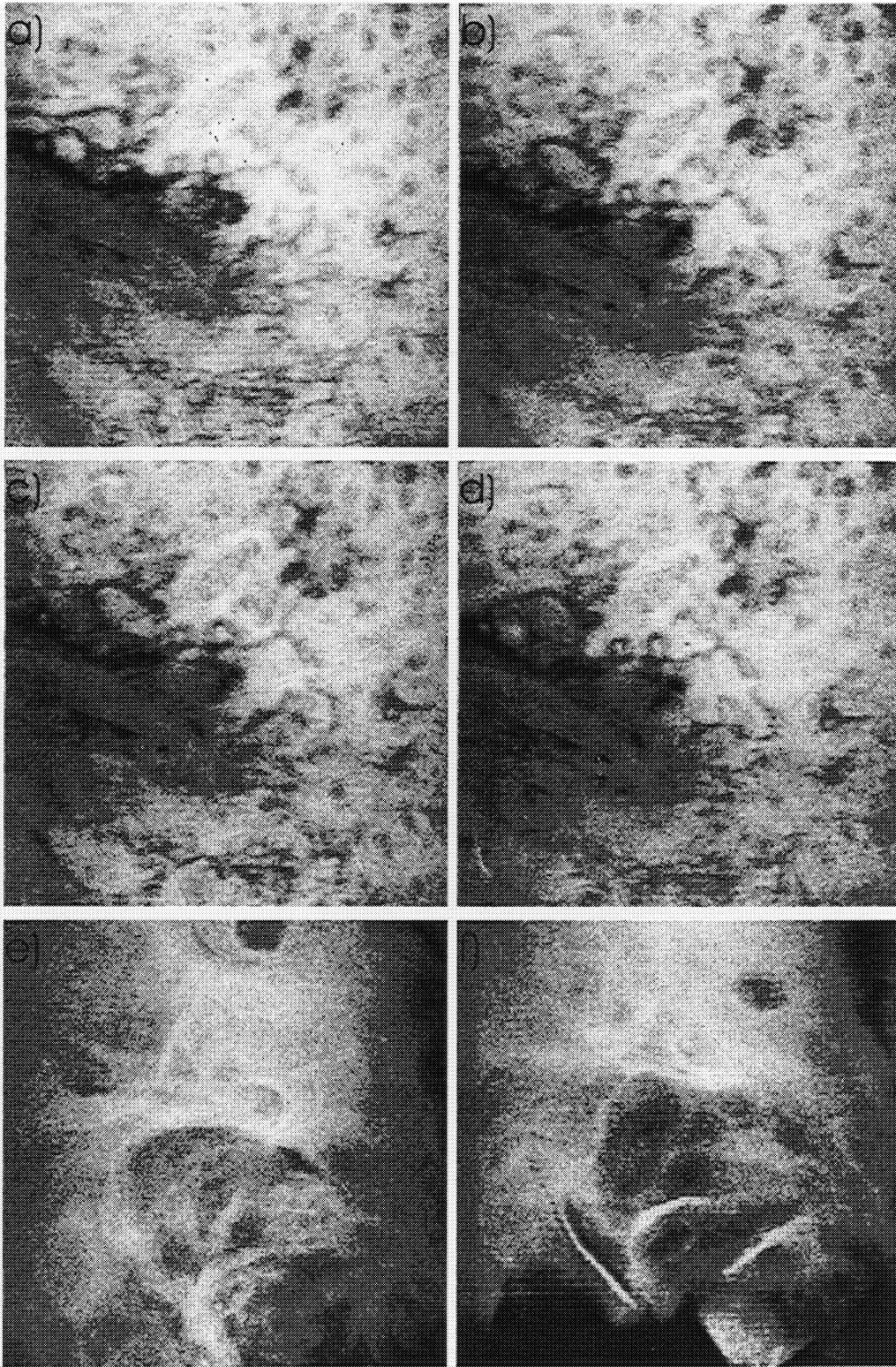
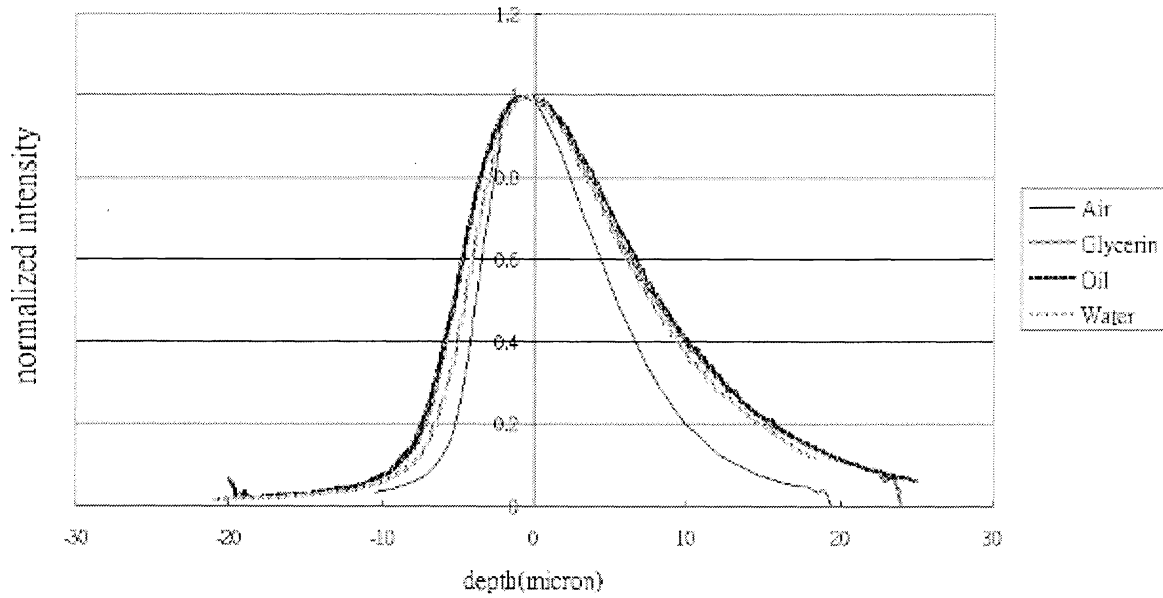


FIG. 5 Skin images. a) 20x air immersion; b) 20x glycerine; c) 20x oil; d) 20x water; e) 60x oil; f) 60x water.

20x skin sample, immersion comparison



60x skin sample immersion comparison

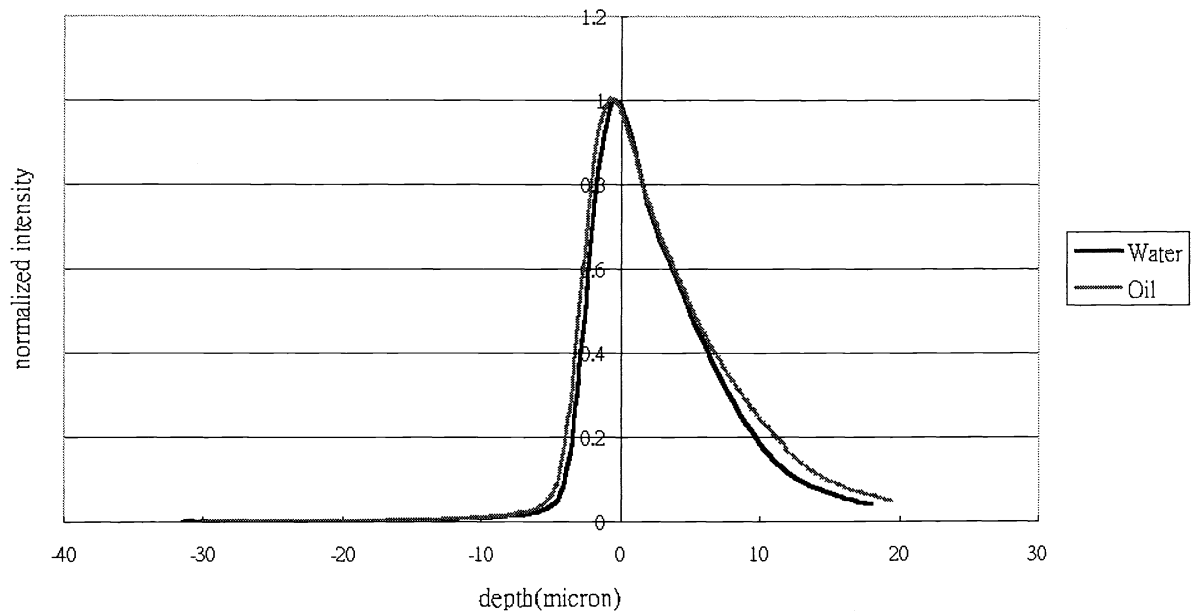


FIG. 6 Depth intensity profiles of the skin sample.